**ACTA IMEKO**
**ISSN: 2221-870X**
*March 2026, Volume 15, Number 1, 1 - 9*

# Attenuation analysis of an underwater optical wireless communication system, based on red light-emitting diodes, in turbid water with preliminary uncertainty analysis

**Giorgia Satta[1], Francesco Pieroni[1], Ruggero de Francesco[2], Fabio Leccese[1]**

[1] *Science Department, Università degli Studi Roma Tre, via della Vasca Navale n.84, 00146 Rome, Italy*
[2] *SeTeL s.r.l, Via Casamari n°6, 00142, Rome, Italy*

ABSTRACT
Underwater communication traditionally relies on acoustic systems, which suffer from high energy consumption, significant latency, and undesirable environmental impact. Optical wireless communication (OWC) technologies represent a promising alternative, yet they are strongly limited by light attenuation in water, especially under turbid conditions. In this work, an innovative low-cost underwater optical wireless communication (UOWC) system based on red LEDs (light-emitting diodes) and photodiodes was developed, allowing not only data transmission, but also experimental characterisation of signal degradation in turbid water. The system was tested by varying the concentration of suspended clay to evaluate the reduction in optical intensity and data transmission rate. Results show a maximum data rate of 1.5 Mbit/s in clear seawater, followed by an exponential decrease in performance as turbidity increases. The proposed approach provides a reproducible and low-cost method for studying the underwater optical channel and represents a foundation for future developments aimed at optimising UOWC systems in more complex and realistic scenarios.

**Section:** RESEARCH PAPER

**Keywords:** UOWC; red light; LED; communication in turbid water; attenuation analysis; Lambert–Beer attenuation law

**Citation:** G. Satta, F. Pieroni, R. de Francesco, F. Leccese, Attenuation analysis of an underwater optical wireless communication system, based on red light-emitting diodes, in turbid water with preliminary uncertainty analysis, Acta IMEKO, vol. 15 (2026) no. 1, pp. 1-9. DOI: 10.21014/actaimeko.v15i1.2255

**Section Editor:** Francesco Lamonaca, University of Calabria, Italy

**Received** November 28, 2025; **In final form** February 22, 2026; **Published** March 2026



**Corresponding author:** Giorgia Satta, e-mail: giorgia.satta@uniroma3.it

## 1. INTRODUCTION

In recent years, there has been growing interest in high-speed, long-range underwater wireless data transmission, aimed at supporting both scientific research activities (such as the monitoring of marine ecosystems, biodiversity, and environmental parameters, as well as geological and geophysical studies) and the development and management of marine infrastructure, including the control and maintenance of offshore installations, the deployment of underwater sensor networks, and communication with autonomous underwater vehicles (AUVs), remotely operated vehicles (ROVs), and marine drones [1]. Traditionally, underwater communication has relied primarily on the use of acoustic waves, as they offer the most effective solution for long-range transmission due to their lower attenuation compared to radio or optical signals [2]. However, acoustic communication presents several limitations, particularly in terms of limited available bandwidth (approximately a few kilohertz), high latency, and strong sensitivity to ambient noise [3].

These constraints introduce delays in data transmission, reducing efficiency in applications that require high data transfer rates and real-time responsiveness. Moreover, the extensive use of acoustic signals may negatively impact the marine ecosystem, contributing to noise pollution and interfering with marine fauna [4]. Finally, in military applications, acoustic communication requires the use of advanced technologies to minimise the risk of interception and ensure the confidentiality of transmitted information [5], [6].

A promising alternative is underwater optical wireless communication (UOWC), which exploits optical signal propagation in water to support high-data-rate communication for underwater sensing applications, including geological and geophysical observations [7], as well as for the monitoring and operation of marine infrastructure [8]. UOWC applications include underwater wireless sensor networks (UWSNs), used for optical interconnection with aerospace and terrestrial systems through the integration of AUVs, ROVs, communication buoys, and satellites [9].

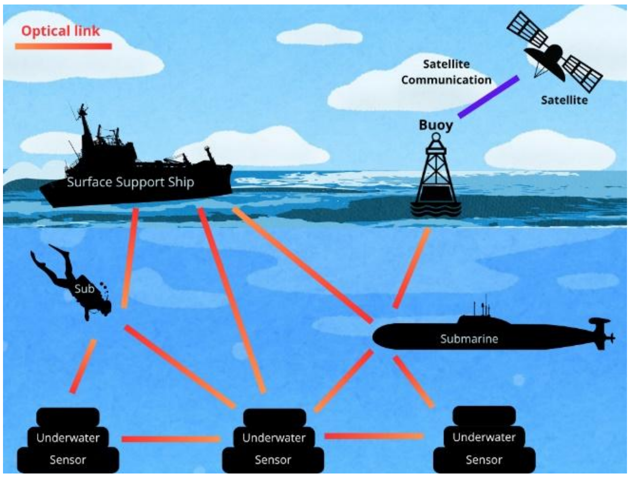


Figure 1. Possible scenario of UOWC application.

Figure 1 shows a possible scenario of an UOWC system supporting high-speed data exchange between submerged sensors, AUVs, and surface stations. The system supports real-time monitoring, infrastructure inspection, and data transmission in marine environments.

Compared to traditional acoustic systems, optical systems offer several advantages, including high bandwidth, low latency, and high data transmission rates, supporting real-time data exchange [9], [10]. These features make them particularly suitable for application scenarios such as AUV control, intensive data collection from sensor networks, and high-definition image or video transmission [11]. Moreover, optical transceivers are generally low-cost and energy-efficient, contributing to a reduced overall environmental impact of the system. Finally, optical systems provide a higher level of security and confidentiality, lowering the risk of interception [12].

Despite its numerous advantages, UOWC has limitations that constrain its widespread use. Notably, the propagation of light in the marine environment is significantly affected by absorption and scattering phenomena, which reduce the effective communication range to a few tens of meters in clear water and just a few meters in turbid or coastal waters [13]. Furthermore, the performance of this technology is highly sensitive to environmental conditions: the presence of suspended particles, phytoplankton, air bubbles, and turbidity can degrade link quality by attenuating the optical signal [14]; ambient light in shallow waters can also cause interference in systems operating within the visible spectrum. Another critical constraint is the requirement for precise alignment between the transmitter and receiver [14], which can be challenging in turbulent underwater environments and may lead to link loss. Finally, the performance and lifespan of optical devices are affected by environmental parameters such as the temperature, pressure, and salinity of seawater [2], [15]. Table 1 summarises the main characteristics of the acoustic and optical systems discussed above.

UOWC therefore represents a technology of significant scientific interest, due to its potential in terms of speed, efficiency, and security [2]. However, the limitations associated with optical signal attenuation in a marine environment and its sensitivity to environmental conditions highlight the need for in-depth research aimed at evaluating its practical applicability and deployment strategies in real-world operational scenarios. The ultimate goal is to define its limitations, optimise system performance, and promote its integration into intelligent underwater infrastructures.

Table 1. Comparison of the main characteristics of acoustic and optical systems in underwater environments.

| Parameter | Acoustic systems | Optical systems |
|---|---|---|
| Bandwidth | Low (kHz) | High (MHz-GHz) |
| Latency | High | Low |
| Energy efficiency | High power required | Lower consumption (LED-based) |
| Security | Weak (wide dispersion) | High (narrow beam) |
| Communication range | > 100 km | < 500 m |

In this context, the present work aims to develop a wireless optical communication system capable of providing high data transmission rates in highly turbid marine environments, such as ports, river mouths, lakes, and aquaculture facilities.

Specifically, a low-cost and environmentally friendly underwater optical prototype has been developed, capable of transmitting data at high speed in clear water, laying the groundwork for its future evolution towards effective operation in turbid waters. Based on a literature review, red light was selected, as it is less harmful to the marine ecosystem and shows a more favourable attenuation coefficient in turbid water than other wavelengths in the visible spectrum [16], [17].

Furthermore, although most underwater optical communication systems focus on high-performance blue LEDs and photodiodes, they are highly vulnerable to turbidity and often require expensive components. In this work, we propose a novel approach based on red LEDs and low-cost photodiodes, designed to ensure reliable data transmission even in the presence of suspended particles. The system allows the experimental evaluation of signal attenuation and transmission speed as a function of clay concentration, providing a quantitative method to characterise the optical channel under realistic conditions.

At the same time, the system has been designed for educational purposes, specifically to enable the experimental verification of the Lambert–Beer attenuation law, providing a real-world context for observing optical propagation in absorbing media such as water.

Thanks to the combination of technology, sustainability, and educational application, this work represents a new low-cost experimental approach for the study of underwater optical communication in turbid scenarios, and provides a starting point for the development of more robust and adaptive systems.

This paper is organised as follows. Section 2 reviews the state of the art on underwater optical communication systems. Section 3 presents the architecture of the proposed system, while Section 4 details the development of the transmitter and receiver modules. Section 5 describes the experimental setup and the test procedures adopted for performance evaluation. The obtained results are reported and discussed in Section 6. Section 7 presents the analysis of the experimental uncertainties, the assessment of measurement repeatability and fit quality. Finally, Section 8 summarises the main conclusions and outlines possible directions for future work.

## 2. STATE OF THE ART

An underwater optical wireless communication system typically consists of three main components: the optical transmitter, the underwater propagation channel, and the optical receiver (Figure 2) [18].

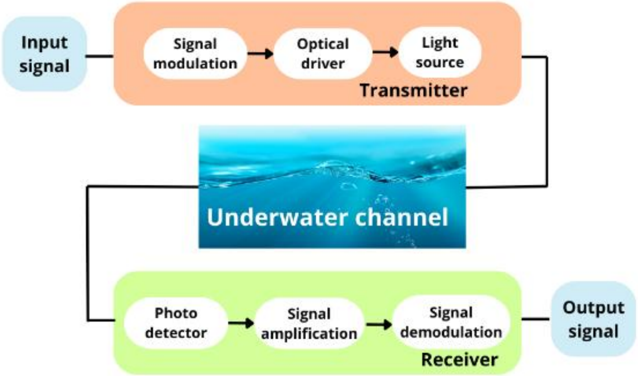


Figure 2. Schematic representation of an underwater optical communication system.

### 2.1. Transmitter

The transmitter is responsible for converting an electrical signal into an optical signal by generating light pulses that are sent into the optical channel. It integrates several subcomponents, including a modulator, a light source, and an optical driver used to drive the light source itself. The choice of modulation technique plays a crucial role in enhancing both the transmission speed and the communication range, given the high attenuation of light in the marine environment. Therefore, it is essential to select the most appropriate modulation scheme based on the specific requirements of the communication system [19].

The light source can consist of either light-emitting diodes (LEDs) or laser diodes (LDs). Laser diodes offer higher bandwidth and optical power, generating coherent radiation. However, due to their narrow divergence angle, they are highly directional and require precise alignment between the transmitter and receiver. For this reason, they are mainly involved in point-to-point communications with a line-of-sight (LOS) configuration, which can be challenging to maintain in marine environments subject to turbulence [18]. Conversely, LEDs emit an incoherent and wide light beam, allowing diffuse LOS communications without the need for strict alignment between the transmitter and receiver [18]. Although they offer lower energy consumption and longer operational lifetime, LEDs have a limited bandwidth, which restricts their use to short-range and low-data-rate communications. Figure 3 shows the typical configurations used with LEDs and laser diodes.

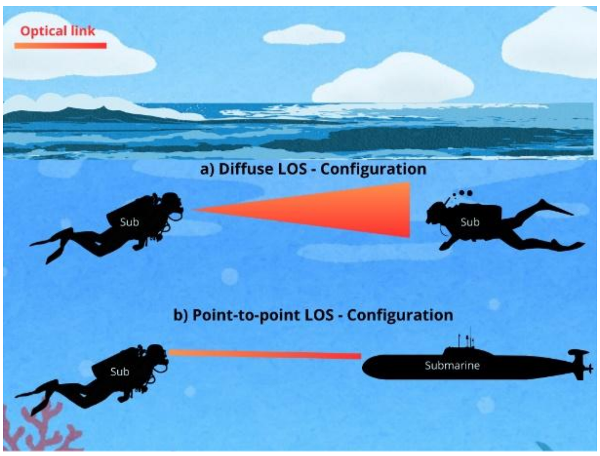


Figure 3. Schematic representation of diffuse LOS configuration used with LEDs and point-to-point LOS configuration employed with laser diodes.

### 2.2. Receiver

The receiver is responsible for detecting the incoming optical signal and for its conversion into an electrical signal. The main element of this process is the photodetector, typically a photodiode, whose selection depends on the performance specifications required by the system, as these devices differ in terms of sensitivity, operating voltage, cost, and size. The most commonly used types include PIN photodiodes and avalanche photodiodes (APDs) [20].

To operate effectively in an underwater environment, the receiver must ensure high sensitivity and substantial gain, to detect weak signals. Moreover, maintaining a high signal-to-noise ratio (SNR) is crucial to ensure accurate decoding of the transmitted information.

### 2.3. Optical channel

The optical channel, represented by the underwater environment, is a highly dispersive and attenuating medium composed of water molecules, suspended and dissolved particles, as well as organic and inorganic components. The interaction of light with these elements causes significant signal attenuation, which can be modelled using the Lambert–Beer law [18]:

$$I = I_0 \, \mathrm{e}^{-c(\lambda)\, d} \,, \tag{1}$$

where $I_0$ and $I$ are the intensity of the incident and outgoing radiation, respectively; $d$ is the optical path, and $c(\lambda)$ is the total attenuation coefficient, defined as the sum of the absorption coefficient $a(\lambda)$ and the scattering coefficient $b(\lambda)$:

$$c(\lambda) = a(\lambda) + b(\lambda) \,. \tag{2}$$

The attenuation of the aquatic medium depends both on the wavelength of the incident radiation and on the optical properties of the water, such as turbidity and the presence of dissolved substances or suspended particles.

Figure 4 [21] shows the absorption and scattering coefficients in pure seawater. For wavelengths within the visible range, the scattering coefficient is almost zero, suggesting that signal attenuation is dominated primarily by absorption [17]. Moreover, the plot highlights that light in the blue-green spectral region (450–550 nm) has the lowest attenuation in seawater compared to other wavelengths.

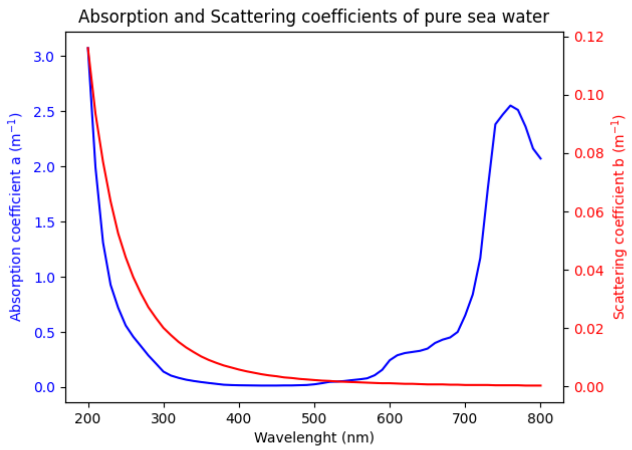


Figure 4. Absorption and scattering coefficients of pure seawater as a function of wavelength. The plot highlights that attenuation in the visible range is dominated by absorption, and that the blue-green region (450–550 nm) exhibits the lowest overall attenuation [18].

However, optical transmission is significantly affected by chlorophyll concentration and turbidity levels, which respectively increase light absorption and scattering. Chlorophyll, a photosynthetic pigment found in algae and phytoplankton, selectively absorbs light in the blue and red bands while predominantly reflecting green light [22]. Its presence enhances spectral absorption, particularly in the blue region, thereby reducing the efficiency of optical transmission at those wavelengths.

Turbidity, on the other hand, is a measure of the concentration of suspended particles in water, and contributes to an increase in the scattering coefficient, leading to greater light diffusion [23]. This phenomenon results in a reduction of the effective communication range, an increase in noise in the received signal, and, overall, a degradation of the optical channel quality.

Different types of water are classified based on their optical properties, that is, on the ability of the water to attenuate or absorb light radiation, depending on the dissolved or suspended particles [24], [25]. The Jerlov classification distinguishes between clear open-ocean waters (types I, IA, IB, II, III) and more turbid coastal waters (types 1–9).

As shown in Figure 5 [26], in clear waters (I, IA, IB, II, III), the attenuation coefficient shows a minimum in the blue wavelength region. As turbidity increases, this minimum progressively shifts towards the green region, eventually reaching the amber wavelengths (approximately 590 nm) in type 9C waters. This behaviour directly reflects the influence of the concentration and nature of suspended particles on light propagation in water.

In turbid waters, such as those found in coastal or harbour areas, or environments with high concentrations of suspended particulate matter, scattering tends to dominate over absorption, making the spectral attenuation coefficient $c(\lambda)$ approximately equivalent to the scattering coefficient $b(\lambda)$. Under these conditions, shorter wavelengths (despite their deeper penetration in clear waters) undergo more pronounced angular scattering, which limits their direct transmission towards the receiver. Since, according to Rayleigh's law, scattering is inversely proportional to the fourth power of the wavelength ($\propto \lambda^{-4}$), light in the red range (600–700 nm) is subject to less diffusion and tends to better preserve beam directionality, enhancing signal concentration at the detector [27]. Moreover, silicon photodiodes, commonly used in underwater optical systems, show high spectral sensitivity in this region [28]. The combination of reduced scattering and increased detector responsivity makes red light particularly effective for short-range optical communications in high-turbidity environments [16].

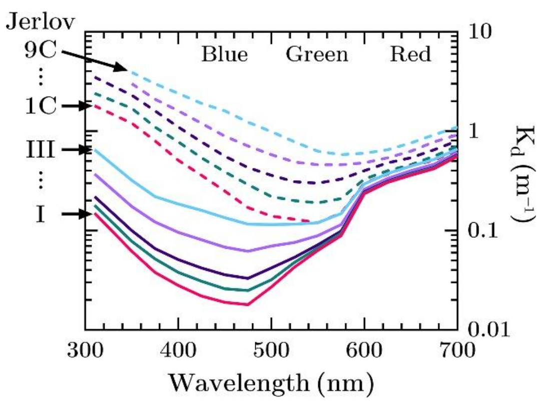


Figure 5. Attenuation coefficient versus wavelength for different Jerlov water types. The minimum shifts from the blue region in clear waters (I–III) to the amber region (~590 nm) in turbid coastal waters (type 9C) [25].

Table 2. Optimal wavelengths for underwater communication according to water type and optical properties.

| Water type | Light used | Reason |
|---|---|---|
| Clear water (ocean, open sea) | Blue-green 450–550 nm | Lower absorption |
| Coastal waters with chlorophyll | Green 520–550 nm | Biological optical window |
| Highly turbid waters (ports, sediments) | Red 600-700 nm | Lower scattering, more directional beam |

Table 2 reports the water types and the corresponding wavelengths to be used.

## 3. DESCRIPTION OF THE PROPOSED SYSTEM

The proposed system is based on optical wireless communication (OWC) for short-range, high-speed underwater applications. A digital system for data transmission and reception has been developed by using on-off keying (OOK) modulation.

The system architecture consists of two main nodes: a transmitting unit and a receiving unit. In this preliminary experimental phase, both units are placed outside the water, with the transmission medium represented by a 33 × 21.4 × 16 cm³ aquarium filled with water, used as the optical channel. Data transmission occurs in an LOS configuration.

The transmitting node consists of an optical driver, a modulator, and an array of six high-power LEDs operating at a wavelength of 625 nm (red), selected for its higher effectiveness in turbid water conditions. The receiving node integrates a photodiode, along with signal amplification and filtering circuits.

A computer via a USB-TTL interface, which allows for modulation frequency configuration and data transmission, manages digital communication. A Python-based application handles the generation and transmission of the data stream to the transmitter, as well as the reception and decoding on the receiving side.

The implementation of this type of transmission was based on the diagram shown in Figure 6.

The system is designed to be low-cost and easily replicable. The use of LEDs ensures high energy efficiency, a long operational lifetime, and a reduced environmental impact compared to alternatives based on high-power laser sources.

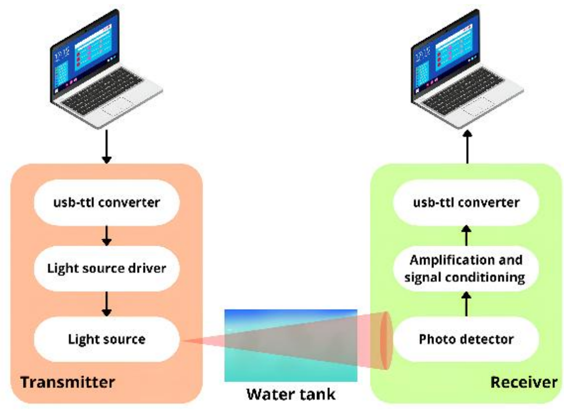


Figure 6. Schematic diagram of the optical wireless communication system used for short-range underwater data transmission. The setup includes the transmitting and receiving units, as well as the optical channel represented by a water-filled aquarium.

## 4. SYSTEM DEVELOPMENT

The main objective of this project was the development of a low-cost, environmentally friendly underwater wireless optical communication system, operating in the red spectral band. This choice makes the system particularly suitable for turbid aquatic environments, such as coastal waters, river mouths, or lakes, where light propagation is significantly limited.

### 4.1. Transmission system

The light source used in the system consists of a cluster of 40 high-power red LEDs (151053RS03000) [29], powered at 12 V through a voltage regulator to ensure a constant and stable light output. Figure 7 shows the electrical circuit designed for the transmission system.

The optical transmitter was implemented using a 5 V TTL digital signal, generated by a computer through a USB–TTL interface, and used as the circuit input. This signal drives an LM311P comparator, considered as an interface between the TTL logic and the power MOSFET. The comparator threshold voltage is set using a 1 MΩ potentiometer, which provides a reference level to the non-inverting terminal. A 0.47 μF capacitor is incorporated into the same network to stabilise the threshold voltage, reduce low-frequency noise, and mitigate transient effects associated with digital switching. The inverting terminal of the LM311P receives the logical input from the TTL–USB converter.

The comparator output, equipped with a 470 Ω pull-up resistor to the 12 V rail, directly drives the gate of the IRF530N MOSFET configured as a switch. In this configuration, the MOSFET allows the commutation of currents significantly higher than those deliverable by the TTL signal, enabling the control of a high-brightness LED array.

The optical load consists of multiple strings of red LEDs, each equipped with a 220 Ω current-limiting resistor. These strings are connected in parallel and powered from the 12 V supply line. The IRF530N operates as an electronically controlled switch driven by the comparator, ensuring fast, stable, and reliable switching of the entire LED array.

This architecture enables the realisation of a robust optical transmitter compatible with TTL digital signals and capable of delivering sufficient optical power for the experiments conducted, while maintaining high immunity to electrical noise thanks to the stabilised comparator threshold and the separation between the control and power stages.

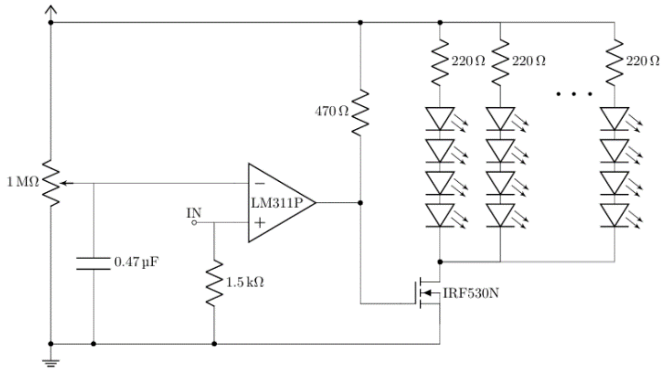


Figure 7. Electrical schematic of the optical transmission circuit, including the TTL-driven LM311P comparator, IRF530N MOSFET switch, and high-power LED array powered at 12 V.

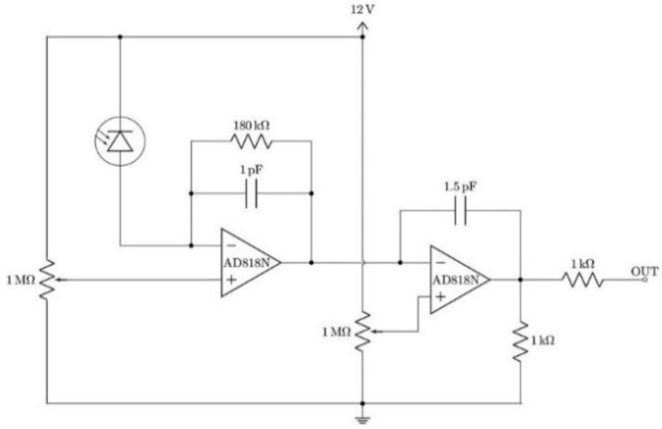


Figure 8. Electrical schematic of the optical receiver, featuring the SFH203 photodiode, the two-stage AD818N transimpedance and amplification stages, and the TTL–USB interface for signal acquisition.

### 4.2. Reception system

Figure 8 shows the electrical circuit designed for the optical reception system.

For the detection of the optical signal, an SFH203 photodiode [30] was considered, selected for its spectral sensitivity and low intrinsic noise. As shown in the circuit, the photodiode is reverse-biased. The photocurrent generated by the sensor is converted into a voltage by a transimpedance amplifier (TIA) based on an AD818N operational amplifier, designed to provide adequate signal amplification and high response linearity. The TIA stage uses a 180 kΩ feedback resistor in parallel with a 1 pF compensation capacitor, a configuration that defines the transimpedance gain and stabilises the frequency response, limiting the useful bandwidth and preventing oscillations.

A 1 MΩ potentiometer is integrated into the amplifier's control network to allow adjustment of the threshold voltage or signal level, supporting compensation for environmental variations such as incident light or changes in water turbidity. A capacitor placed in the conditioning network (as highlighted in the schematic) helps to damp threshold voltage fluctuations, reducing low-frequency noise and transient effects.

The output signal from the TIA is fed into a second conditioning stage, also based on an AD818N, which provides additional amplification and impedance matching for the acquisition circuitry. This stage includes a feedback network with a 1.5 pF capacitor and an output resistor of 1 kΩ, which together shape the frequency response and stabilise the DC level. A second 1 MΩ potentiometer on the input path of this stage allows further adjustment of the operating point (offset).

The final output is isolated through a 1 kΩ output resistor and delivered to a TTL–USB converter for digitisation and transfer to the computer for data acquisition and numerical processing. This interface requires a properly conditioned logic-level signal; the output resistor protects the operational amplifier from external loads and limits accidental short-circuit currents.

Overall, the two-stage architecture ensures a linear conversion of photocurrent into voltage, effective noise mitigation, and flexible adjustment of the operating point. This configuration provides stable and reliable optical signal reception, even in the presence of fluctuations in light intensity or variable experimental conditions such as water turbidity, while maintaining the linearity required for subsequent quantitative data analysis.

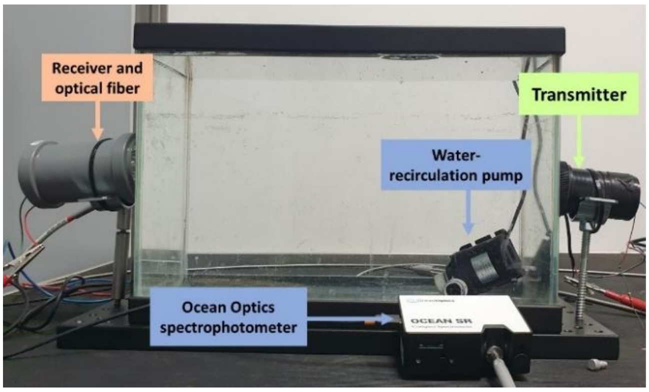


Figure 9. Experimental setup showing the aquarium with clear water. The transmitter and receiver are visible, together with the water-recirculation pump that ensures uniform conditions inside the tank. The spectrophotometer is positioned to monitor the optical intensity during the measurements.

## 5. EXPERIMENTAL TEST

The system was initially validated in air and subsequently tested in an underwater environment using an aquarium containing approximately 11.3 litres of water under static conditions. The transmitted and received signals were monitored in real time on a PC. Under these conditions, the system achieved a data transmission rate of Mbit/s, operating at a modulation frequency of 1.5 MHz.

Figure 9 shows the experimental setup in clear water. The transmitter and receiver are visible, along with the water-recirculation pump and the spectrophotometer used to measure the optical intensity.

To simulate seawater salinity, 395.5 g of NaCl were dissolved in the aquarium water, corresponding to a concentration of 35 g/l, representative of the average ocean salinity [31]. Subsequently, varying amounts of clay were added to reproduce different turbidity levels.

Table 3 reports the clay concentrations introduced into the aquarium during the various measurements.

To prevent particle sedimentation and ensure a homogeneous suspension, a continuous recirculation hydraulic pump was employed. This setup also allowed the simulation of turbulence conditions typical of the marine environment. In the laboratory tests, the data transmission rate and the optical signal intensity were evaluated as a function of different water turbidity levels.

The measurements of the light intensity emitted by the LEDs were carried out using an SR6 Ocean Optics spectrophotometer [29], featuring a spectral range of 180–1100 nm and a resolution of 0.36–11.52 nm, and interfaced with its dedicated acquisition and analysis software. Light was collected through a multimode optical fibre (400 µm core diameter), which ensured efficient coupling from the source while minimizing alignment sensitivity. This setup allowed an accurate monitoring of the optical power at the transmitter side, supporting the validation of the

Table 3. Clay concentrations for the different measurement conditions.

| Clay (g) | Clay concentration (mg/l) |
|---|---|
| 0.32 | 30 |
| 0.42 | 40 |
| 0.53 | 50 |
| 0.82 | 70 |

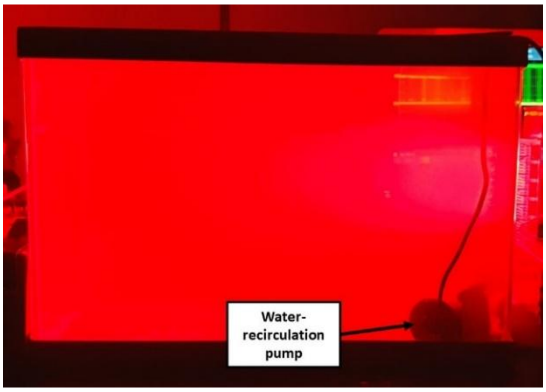


Figure 10. Optical transmission using red LEDs inside the aquarium at maximum clay concentration. The water-recirculation pump is also visible.

attenuation behaviour of both the emitted signal and the light intensity detected by the receiver as the concentration of suspended clay increased.

Figure 10 shows the optical transmission using red LEDs inside the aquarium under the condition of maximum clay concentration. The water-recirculation pump, used to maintain a homogeneous suspension, is also visible.

## 6. RESULTS

Data analysis was carried out to evaluate the transmission rate of the developed optical communication system under turbid water conditions. For this purpose, a Python-based script was implemented for the graphical processing of the experimental data and for an exponential regression analysis, aimed at describing the relationships between the transmission rate and signal attenuation as a function of turbidity level.

Figure 11 shows the emission spectrum of the red LEDs, acquired using an Ocean Optics spectrophotometer [32]. The main emission peak is centred around 635 nm, in accordance with the device specifications.

Spectral analysis highlights that, as the clay concentration (and consequently the water turbidity) increases, a progressive reduction in the emission peak intensity occurs. This behaviour is consistent with the increase in optical attenuation caused by

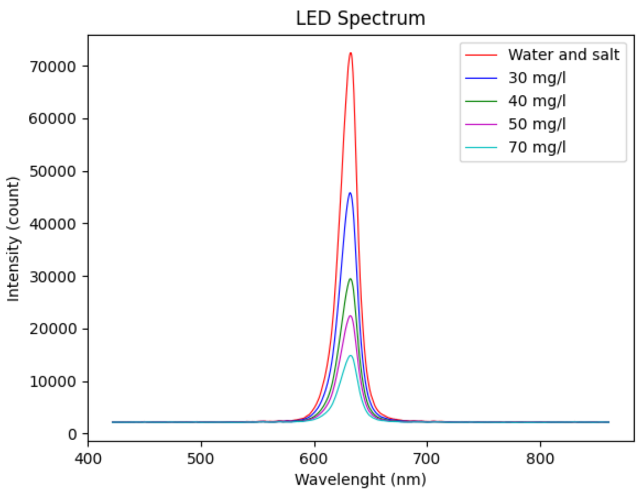


Figure 11. Emission spectrum of the red LEDs measured with an Ocean Optics spectrophotometer. The main peak is centred around 635 nm, consistent with the device specifications. A decrease in emission intensity is observed with increasing clay concentration, indicating enhanced optical attenuation due to scattering and absorption effects.

scattering and absorption phenomena induced by suspended particles, which reduce the amount of light transmitted through the medium. The decrease amounts to approximately 80 % between the clearest and the most turbid samples.

Subsequently, the light intensity values were analysed as a function of clay concentration to verify the validity of the Beer–Lambert attenuation law.

According to this law, the intensity of the light radiation III transmitted through a turbid medium is described by the equation:

$$I = I_0 \,\mathrm{e}^{-\alpha C} , \tag{3}$$

where $I_0$ is the initial system intensity in clear water, $C$ is the clay concentration, and $\alpha$ is the attenuation coefficient accounting for light absorption and scattering within the medium.

The experimental data (Figure 12) show a decreasing exponential trend of light intensity with increasing turbidity, in accordance with the theoretical model. The exponential regression analysis provided a coefficient of determination ($R^2$) of 97 %, confirming the high reliability of the Beer–Lambert law in describing the attenuation of light radiation as a function of clay concentration.

As observed for light intensity, the data analysis highlighted that the system's transmission rate decreases exponentially with increasing turbidity, as shown in Figure 13. This behaviour can be attributed to the higher optical signal attenuation caused by light scattering and absorption from suspended clay particles.

Since the transmission rate is related to the signal-to-noise ratio (SNR), which is in turn directly proportional to the received optical power, the observed relationship can be described by the following equation:

$$v = v_0 \,\mathrm{e}^{-\alpha C} , \tag{4}$$

where $v_0$ is the initial system transmission rate in clear water. The coefficient of determination ($R^2 = 0.99$) confirms the goodness of fit and the validity of the proposed model.

## 7. UNCERTAINTY ANALYSIS

The proposed system shows that the transmission rate reaches 1.5 Mbit/s in clear water, and that its decrease with increasing turbidity follows an exponential trend, consistent with what is observed for the light intensity. The setup was not designed to achieve high-precision measurements, but rather to

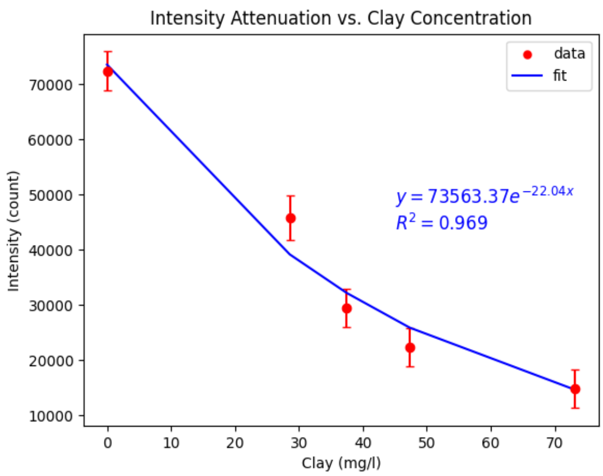


Figure 12. Exponential decay of light intensity as a function of clay concentration, fitted according to the Beer–Lambert law.

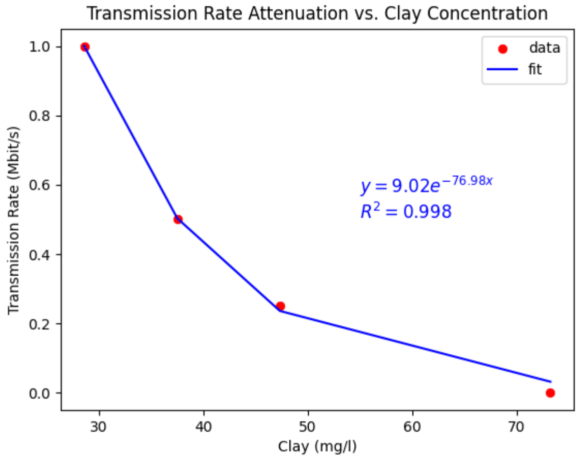


Figure 13. Exponential decrease of data transmission rate as a function of water turbidity.

reliably assess the behaviour of data transmission as the conditions of the optical channel vary. The uncertainties associated with the transmission system (photodiode sensitivity, LED optical power, possible fluctuations in the supply voltage, stability of the digital signal) and with the receiving system (electronic noise, amplifier stability, alignment variability) are overall smaller than the uncertainties introduced by the experimental setup, particularly those related to the properties of the optical channel itself and to the system geometry.

In this context, different concentrations of clay were introduced to simulate various turbidity levels and the resulting changes in light-propagation conditions, also due to refractive-index variations introduced by suspended particles. In addition, possible reflections from the aquarium walls, turbulence, and air bubbles generated by the recirculation pump should be taken into account. All these factors represent the main source of uncertainty and dominantly affect the measurement of the transmission rate and of the light intensity.

The experimental setup was designed to obtain repeatable measurements under identical conditions:

- The turbidity is controlled through known clay concentrations;
- The system geometry, i.e., the transmitter–receiver distance and alignment, is kept fixed;
- Measurements were taken in darkness to minimise ambient-light noise.

To best evaluate the system performance, five measurements of the light intensity were carried out for each turbidity level using the optical fibre and spectrophotometer, to minimise counting fluctuations and assess the signal stability. Repeating the acquisitions allowed us to reduce the influence of statistical noise and of possible variations related to optical sampling.

Conversely, since the transmission rate does not show continuous fluctuations but varies in discrete steps determined by the modulation protocol, the data-rate measurement was carried out only once for each turbidity level. Repeating the measurement would not have provided significant benefits in terms of reducing statistical uncertainty.

The quality of the fits (Figure 12 and Figure 13) demonstrates that the system is stable, confirming the exponential trend predicted by the Lambert–Beer law and the reliability of the measurements.

## 8. CONCLUSION

Underwater optical communication systems represent a low-cost alternative for transmissions in marine environments. In this work, an LED-based system was developed to investigate signal degradation as a function of water turbidity.

Experimental tests confirmed the feasibility of low-power, low-cost optical transmissions, achieving data rates on the order of Mbps in seawater, with performance decreasing as turbidity increased. The collected data provide a solid foundation for further developments aimed at optimising the system in complex and dynamic underwater scenarios, as well as for a more in-depth study of the optical channel.

The use of red LEDs and photodiodes proved effective in controlled environments; however, the observed exponential behaviour indicates that even small variations in turbidity can significantly reduce channel capacity, limiting optical communication performance. The innovation of the proposed system lies in its ability to experimentally characterise the optical channel under realistic conditions, providing a low-cost and reproducible approach for studying optical propagation in turbid water.

Future work will focus on extending the experimental campaign through a larger set of controlled measurements, including a wider range of turbidity levels and transmission distances, to improve the statistical characterisation of the optical channel. Additional investigations will address the evaluation of different system configurations, such as alternative optical wavelengths and receiver sensitivities, as well as the measurement of further physical-layer performance metrics, including bit error rate and signal-to-noise ratio. Moreover, dedicated measurements will be conducted to achieve a more detailed characterisation of the optical channel, including absorption, scattering, and noise contributions. These experimental activities will contribute to a more accurate empirical modelling of optical signal propagation in turbid water, and to the identification of the operational limits of low-cost underwater optical communication systems.

## AUTHORS' CONTRIBUTION

Conceptualization: G.S.; methodology: G.S. and F.P.; validation: L.R. and R.D.F.; formal analysis: G.S.; investigation: G.S. and F.P.; resources: F.L; data curation: G.S.; writing—original draft preparation: G.S.; writing—review and editing: F.L.; supervision: F.L and R.D.F. All authors have read and agreed to the published version of the manuscript.

## REFERENCES


[1] Z. Li, W. Li, K. Sun, D. Fan, W. Cui, Recent Progress on Underwater Wireless Communication Methods and Applications, J. Mar. Sci. Eng. 13 (2025) 8, p. 1505. DOI: 10.3390/jmse13081505

[2] S. Zhu, X. Chen, X. Liu, G. Zhang, P. Tian, Recent progress in and perspectives of underwater wireless optical communication, Progress in Quantum Electronics 73 (2020), p. 100274. DOI: 10.1016/j.pquantelec.2020.100274.

[3] M. Stojanovic, J. Preisig, Underwater acoustic communication channels: Propagation models and statistical characterization, IEEE Communications Magazine, vol. 47, no. 1, January 2009, pp. 84-89. DOI: 10.1109/MCOM.2009.4752682

[4] C. Peng, X. Zhao, G. Liu, Noise in the Sea and Its Impacts on Marine Organisms, Int. J. Environ. Res. Public Health 12 (2015) 10, pp. 12304-12323. DOI: 10.3390/ijerph121012304

[5] R. Diamant, L. Lampe, Low Probability of Detection for Underwater Acoustic Communication: A Review, IEEE Access, vol. 6, 2018, pp. 19099-19112. DOI: 10.1109/ACCESS.2018.2818110.

[6] A. F. Gentile, D. Macrì, D. L. Carnì, E. Greco, F. Lamonaca, A Network Performance Analysis of MQTT Security Protocols with Constrained Hardware in the Dark Net for DMS, Applied Sciences 14 (2024) 18, 8501. DOI: 10.3390/app14188501

[7] A. Vitale, F. Lamonaca, Enhancing GeoAI land cover classification via hyperparameter tuning and cross-validation: A case study in Ravenna, Italy, Measurement 257 (2026) Part A, pp. 1-19. DOI: 10.1016/j.measurement.2025.118662

[8] D. L. Carni, C. Scuro, F. Lamonaca, R. S. Olivito, D. Grimaldi, Damage analysis of concrete structures by means of B-value technique, Computing International Scientific Journal 16 (2017) 2, pp. 82-88. DOI: 10.47839/ijc.16.2.884

[9] G. Schirripa Spagnolo, L. Cozzella, F. Leccese, Underwater Optical Wireless Communications: Overview, Sensors 20 (2020) 8, 2261. DOI: 10.3390/s20082261

[10] C. Fang, S. Li, Y. Wang, K. Wang, High-Speed Underwater Optical Wireless Communication with Advanced Signal Processing Methods Survey, Photonics 10 (2023) 7, 811. DOI: 10.3390/photonics10070811

[11] D. Jung, R. Zhang, H. Cho, D. Ji, S. Kim, H. Choi, Control and Real-Time Monitoring of Autonomous Underwater Vehicle Through Underwater Wireless Optical Communication, Appl. Sci. 15 (2025) 11, 5910. DOI: 10.3390/app15115910

[12] F. Leccese, G. Schirripa Spagnolo, LED-to-LED wireless communication between divers, Acta IMEKO 10 (2021) 4, pp. 80-89. DOI: http://doi.org/10.21014/acta_imeko.v10i4.1177 .

[13] S. A. Adnan, H. A. Hassan, A. Alchalaby, A. C. Kadhim, Experimental study of underwater wireless optical communication from clean water to turbid harbor under various conditions, International Journal of Design & Nature and Ecodynamics 16 (2021) 2, pp. 219-226. DOI: 10.18280/ijdne.160212

[14] G. Schirripa Spagnolo, L. Cozzella, F. Leccese, A Brief Survey on Underwater Optical Wireless Communications, MetroSea 2020 - TC19 Int. Workshop on Metrology for the Sea, Naples, Italy, 5-7 October 2020, pp. 79-84. Online [Accessed 16 March 2026] https://www.imeko.org/publications/tc19-Metrosea-2020/IMEKO-TC19-MetroSea-2020-15.pdf

[15] H. Yuan, M. Kong, M. Wang, W. Cui, Y. Pan, H. Zhou, Q. Yang, Effect of turbulence-induced sediment resuspension and sedimentation on underwater wireless optical communication, Opt Express 32 (2024) 9, pp. 16292-16306. DOI: 10.1364/OE.519243

[16] G. Satta, G. Schirripa Spagnolo, E. De Francesco, L. Rampini, F. Pieroni, F. Leccese, Red light in underwater measurement applications: a short review. Acta IMEKO 14 (2025) 2, pp. 1-10. DOI: 10.21014/actaimeko.v14i2.2090

[17] G. Schirripa Spagnolo, G. Satta, F. Leccese, LEDs for Underwater Optical Wireless Communication, Photonics 12 (2025) 8, 749. DOI: 10.3390/photonics12080749

[18] H. Kaushal, G. Kaddoum, Underwater Optical Wireless Communication, IEEE Access 4 (2016), pp. 1518-1547. DOI: 10.1109/ACCESS.2016.2552538

[19] M. M. Zayed, M. Shokair, Performance analysis and optimization of modulation techniques for underwater optical wireless communication in varied aquatic environments, Sci Rep. 15 (2025), 32570. DOI: 10.1038/s41598-025-18406-y

[20] F. Leccese, G. Schirripa Spagnolo, State-of-the art and perspectives of underwater optical wireless communications, Acta IMEKO 10 (2021) 4, pp. 25-35.
DOI: 10.21014/acta_imeko.v10i4.1097
[21] R. Smith, K. Baker, Optical properties of the clearest natural waters (200–800 nm), Appl. Opt. 20 (1981) 2, pp. 177-184.
DOI: 10.1364/AO.20.000177
[22] F. Fina, F. Leccese, The LED's spectrophotometry in precision agriculture: A brief survey, Acta IMEKO 14 (2025) 1, pp. 1-15
DOI: 10.21014/actaimeko.v14i1.1970
[23] B. G. Kitchener, J. Wainwright, A. J. Parsons, A review of the principles of turbidity measurement, Progress in Physical Geography: Earth and Environment, 41 (2017) 5, pp. 620-642.
DOI: 10.1177/0309133317726540
[24] N. G. Jerlov, Classification of sea water in terms of quanta irradiance, Journal du Conseil 37 (1977) 3, pp. 281-287,
DOI: 10.1093/icesjms/37.3.281
[25] P. M. Moser, Spectral transmission of light through seawater. Online (Accessed 16 November 2025]
https://apps.dtic.mil/sti/tr/pdf/AD1012965.pdf
[26] A. Morel, L. Prieur, Analysis of variations in ocean color, Limnol. Oceanogr. 22 (1977) 4, pp. 709-722.
DOI: 10.4319/lo.1977.22.4.0709
[27] K. Sun, Y. Li, Z. Han, Research on Underwater Wireless Optical Communication Channel Model and Its Application, Applied Sciences 14 (2024) 1, 206.
DOI: 10.3390/app14010206
[28] N. Almaymoni, O. Alkhazragi, W. H. Gunawan, G. Melinte, T. K. Ng, B. S. Ooi, High-Speed 645-nm VCSELs for Low Scattering-Loss Gb/s Underwater Wireless Optical Communications, IEEE Photonics Technology Letters 36 (2024) 6, pp. 377-380.
DOI: 10.1109/LPT.2024.3360229
[29] Würth Elektronik, 151053RS03000 datasheet. Online [Accessed 25 January 2026]
https://docs.rs-online.com/180a/0900766b81302e66.pdf
[30] OSRAM, SFH 203 datasheet. Online [Accessed 25 January 2026]
https://docs.rs-online.com/9f58/0900766b816d8a09.pdf
[31] D. Patil, P. P. Gohil, H. Desai, Analysis of Seawater Quality Parameter and Treatment with Hydrodynamic Cavitation Method, 2024
DOI: 10.48550/arXiv.2407.07115
[32] Oceanoptics, SR6 datasheet. Online [Accessed 22 November 2025]
https://www.oceanoptics.com/spectrometers/versatile-spectrometers/